Proceedings of the 21st ICSMGE, Vienna, Austria, 14 – 19 June 2026. Pistrol, Adam & Schweiger (eds.)
Published by: ÖGG, Austrian Society for Geomechanics, Salzburg, Austria, ISBN 978-3-9503898-4-5
https://doi.org/10.53243/ICSMGE2026-2159

Lessons learnt from a highway embankment failure on column-stabilized soft ground

Frank Rackwitz, Daniel Aubram, Melina Gralle
TU Berlin, Chair of Soil Mechanics and Geotechnical Engineering, Germany, frank.rackwitz@tu-berlin.de

Maik Schüßler
HWR Berlin, Germany

Ralf Glasenapp
BHT Berlin, Germany

ABSTRACT: The highway BAB A 20 crosses the marshland of the river Trebel about 40 km east of the city of Rostock. In October 2017 and in January/February 2018 a ground failure of the embankment occurred on a total length of about 80 m. In the years 2001/2002 during the construction of the new BAB A 20 in this area about 80,000 CSV columns (combined soil stabilization with vertical columns) with a total length of about 641,000 m has been installed to stabilize the soft soils consisting of peat and organic soils. In 2005 the new four-lane highway was opened to traffic in the same area. As part of a research project initiated by the Federal Highway Research Institute (BASt), the TU Berlin carried out a scientific assessment of the case of damage. In addition to the review of the literature and the documents relating to the planning and execution of the construction project, experimental investigations were carried out both in the field and in the laboratory. Model tests provided insights into the hydration behaviour of the stabilizing columns. Analytical and numerical calculations, the latter using sophisticated constitutive models for the soft soils, were performed in addition to the experimental tests. Parameter variations in the calculations provided insides into the failure mechanisms of the embankment. The results are compared with the available data from the studied documents, such as in situ measurements of vertical and horizontal soil deformations during and after construction. The main findings from the scientific investigations to determine the causes of the damage and the lessons learnt for future planning and design of embankments on stabilized soft soils are presented.

KEYWORDS: forensic geotechnical engineering, highway embankment failure, organic soils, rigid inclusions, ground improvement.

1 INTRODUCTION

The German federal highway (BAB) A 20 was built as part of the 'German Unity Transport Projects', running east-west almost parallel to the Baltic Sea coast. Approximately 40 km east of Rostock, the BAB A 20 crosses the Trebelniederung moorland over a length of about 1.4 km with a 530 m long viaduct and connecting embankments totalling 870 m (Figure 1). The four-lane motorway was opened to traffic in this area in 2005.

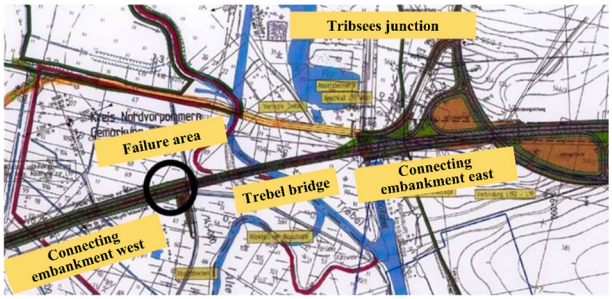

Figure 1. Overview map of the BAB A 20 highway with the failure area 2017/2018 circled (after Hecht, 2010)

Due to detected and measured vertical subsidence of the road surface west of the Trebel bridge, the left lane in the direction of Lübeck was closed. On October 9, 2017, the embankment structure failed over a length of approx. 40 m (1st failure in Figure 2) and the highway was completely closed. Another fracture appeared in the left lane during the night of January 31 to February 1, 2018 (2nd failure in Figure 2). A third failure occurred in the opposite right lane in the direction of Szczecin during the night of February 11 to 12, 2018 (Figure 2). The German Federal Highway Institute (BASt) commissioned the Technische Universität Berlin (TU Berlin) to conduct a scientific investigation and assessment of the damage. However, this research project started after the western embankment structure, including the damaged area, had been completely dismantled. The key findings of these investigations are presented below.

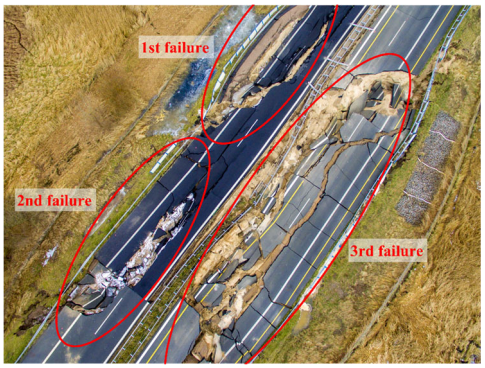

Figure 2. Damaged areas west of the Trebel bridge (Image source: OSTSEE-Zeitung / Alexander Müller)

2 GROUND CONDITIONS

Figure 3 shows a longitudinal section of the subsoil in the area of the damaged section after the first fracture occurred. Underneath the existing embankment structure lies a Holocene lowland peat deposit consisting mainly of moderately to heavily decomposed peat with thicknesses of up to 4 m. Below this are mostly sedimented muds with a thickness of approx. 2 m in the damaged area, consisting mainly of detrital muds and limestone muds, with occasional silt muds. In the damaged area, the peat and mud are underlain by up to 2 m of organogenic silt, followed by up to 5 m of clay. Below these soft soils lie Pleistocene sands with interlayers of boulder clay.

In 2019, two boreholes (diameter 219 mm) were drilled approx. 150 m west of the damaged area, reaching a depth of around 13 m below ground level, in order to examine the subsoil conditions.

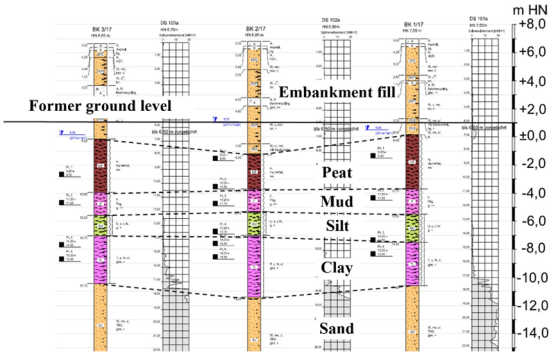

Figure 3. Longitudinal section of the subsoil in the damaged area, lane heading towards Szczecin (after Rackwitz et al. 2021).

The ranges of the corresponding classification parameters determined at TU Berlin are listed in Table 1. Overall, these characteristic values confirm the results of previous studies conducted as part of the project. Further investigations into undrained cohesion revealed minor deviations towards the unfavorable end of the scale. However, the determined drained shear parameters φ' and c' were within the safe range compared with the earlier investigation data (Rackwitz et al. 2021).

Table 1. Soil classification parameters for undisturbed samples

Soil parameters	Peat	Mud	Silt / Clay
Water content, w_n [m.%]	594 … 766	52 … 189	24 … 29
Void ratio, e [/]	11.2 … 13.8	1.57 … 4.9	0.64 … 0.76
Loss on ignition, V_{gl} [m.%]	62 … 85	3 … 9	3 … 5
Lime content, V_{Ca} [m.%]	0.8 … 1.7	82 … 91	20 … 59

The Trebel river flows through the central area of the valley and is the main watercourse, supplying the peat deposit with water. The peat deposit forms the uppermost water-bearing layer. In the failure area, the free groundwater level was found to range from 0.5 to 0.8 m HN (former ground level ~1.0 m HN, Figure 3) in 2001 and 2017. The underlying mud, organogenic silts and clays have very low groundwater conductivity or are impermeable to water, forming a hydraulic barrier between the peat and the lower sands. The lower sand layers form the main groundwater level over a large area with a strong groundwater gradient from the adjacent plateau to the Trebelniederung.

Groundwater in a moor can contain calcium-dissolving carbonic acid, free mineral acids, humic acids and sulfates, which can attack concrete and influence its setting behaviour. In 2019, water from the peat area was analyzed chemically at TU Berlin, but no corrosive effect on concrete was observed.

3 FOUNDATION OF THE EMBANKMENT

The commissioning of the embankment structure's foundation was based on a partial-functional performance specification. Therefore, the foundation had to comply with the boundary conditions of the planning approval process, which included minimal to no compression of the moor subsoil and no full soil replacement. The method of soil improvement using CSV columns (Combined Soil Stabilization with Vertical Columns) (DGGT e.V. 2002; Scheller & Reitmeier 2001) as rigid inclusions fundamentally fulfilled these requirements. During the construction of the BAB A 20 highway, approx. 80,000 CSV columns were installed as planned in the area of the Trebel crossing. An further 7,000 columns, totalling around 700,000 m in length, were installed in the subsoil for the embankment foundation. The installation principle is shown in Figure 4.

The CSV columns were installed as dry mortar columns from a working layer. According to the documentation, they were constructed with a diameter of at least 15 cm and arranged in a square grid with spacing of approx. 0.7 to 1.2 m.

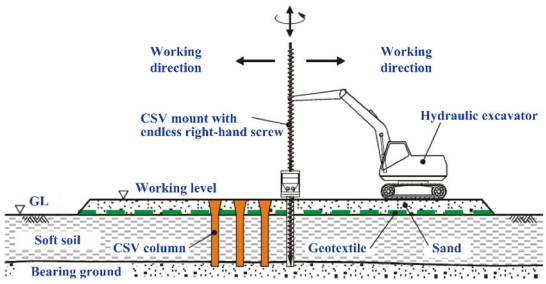

Figure 4. Installation principle of CSV columns

The length of the columns was chosen so that they would penetrate into the load-bearing soil beneath the soft layers of the moor. To limit horizontal deformations resulting from the spreading stresses occurring at the embankment base, a binder-improved and geosynthetic-reinforced layer was placed above the column heads. Vertical (VIC) and horizontal inclinometers (HIC) were installed and geodetic measuring points were set up to monitor the deformations. (Figure 5)

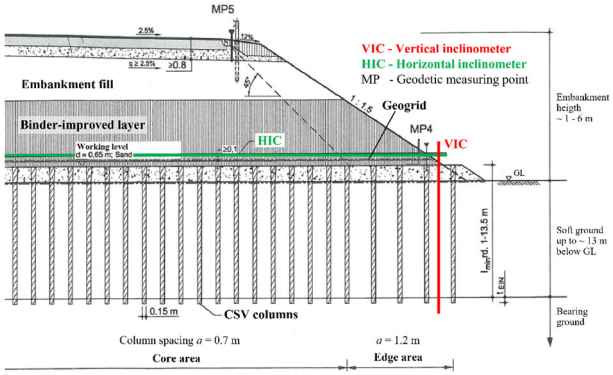

Figure 5. Principle cross-section of the BAB A 20 embankment structure showing the measuring equipment (after Rackwitz et al. 2021)

CSV columns are slender, unreinforced support elements that are hydraulically bound. The material used was a dry granulate consisting of 25% CEM I 42.5 R and 75% sand with a grain size of 0-4 mm. This cement is characterised by high hydration heat, high early strength and normal post-hardening. To check the arrangement and condition of the CSV columns, an excavator trench was dug and columns were recovered using the overdrilling method. As this method only allows for piece-by-piece recovery, it was not possible to make a statement about the in situ integrity of the columns. The location of the columns in the floor plan did not correspond to the existing documents.

The column diameters were determined from these pieces and additional column remains from 2018, which were recovered during the construction of bored piles for a temporary bridge foundation. The determined average values for all soil layers revealed that the planned diameter of at least 15 cm was achieved over the entire column lengths. The cylindrical and cubic compressive strength was determined by testing over 80 individual samples taken from the recovered column pieces and remains. The results confirmed the expected correlation between compressive strength and bulk density. Mean values ranged from 20 N/mm² at 1.9 g/cm³ to 70 N/mm² at 2.3 g/cm³, showing an almost linear trend.

Following the failure, the embankment structure was completely dismantled by May 2018 to an elevation of 2.3 m HN. In the area of the Trebel crossing, the BAB A 20 highway was constructed using asphalt with a 26 cm thick bituminous surface on a hydraulically bound base layer. In 2015 and 2016, maintenance measures were carried out on the superstructure in the area of the subsequent damage. According to the available investigation results, the asphalt layer thickness was increased to

35 cm (lane towards Szczecin) and 50 cm (lane towards Lübeck). These measures therefore compensated for vertical deformations of up to 24 cm.

The substructure was designed in two parts (Figure 5): a binder-improved soil package with a upper edge at 3.72 m HN and unbound embankment fill materials above it. During the dismantling in the failure area, the upper edge of the binder-improved layer was found to be between 2.1 and 3.6 m HN. According to the available documentation, the layer was installed with insufficient thickness. However, a reliable assessment of the embankment structure and the binder-improved layer was not possible due to incomplete documentation.

After covering the ground level with a fleece and a geotextile, a sand fill with a planned thickness of 0.65 m was constructed as the working level (Figure 4 and Figure 5). Due to the high compressibility of the peat, application of the sand fill inevitably resulted in settlement. To ensure the quality of the CSV columns, additional sand fill was used to compensate for this settlement and maintain a consistent upper edge to the working level. Furthermore, the planning documents specified a 0.2 m-thick leveling fill between the column heads and the binder-improved layer. During the drilling in 2017, it was found that the actual thickness of the working level ranged from 1.5 to 2.95 m, significantly more than the planned 0.65 m.

4 DEFORMATION MEASUREMENTS

Seven measuring cross-sections with vertical (VIC) and horizontal inclinometers (HIC) were set up in the Trebelniederung area to monitor the horizontal and vertical deformation of the embankment and the subsoil (Figure 5). Measurements began in May 2002, before the embankment was filled, and were completed in November 2004. Following the detection of deformations in the road surface, VIC measurements were resumed in June 2017 and the road surface was geodetically monitored.

Figure 6 shows the embankment settlement measured by the HIC at km 144+926 in the area of subsequent failure, up to two years after the embankment completion. At this cross-section, the measuring tube was installed at an approx. height of +2.2 m HN. The greatest vertical deformations occurred after two years of service, reaching 59 mm at the centre of the embankment. These deformations decreased towards the edges, with lower settlements measured in the southern (right) part of the embankment cross-section than in the northern (left) part. According to the installation protocols for the CSV columns in this embankment section, additional 494 columns were installed between those already constructed as part of a remediation concept. Most of these additional columns were installed under the right-hand lane in the southern part, which explains the lower deformations, as the column spacing is denser there.

Figure 6. HIC measurements of km 144+926 in the failure area at a height of +2.2 m HN

Two years after completion of the embankment structure, maximum VIC head deformations of between 29 and 100 mm were measured across all cross-sections, with the largest occurring in the subsequent failure area. Discrepancies between the evaluated VIC head deformations and the geodetic measurements of the inclinometer tube heads from 2017 indicated unwanted displacement at the foot of the tubes. Figure 7 shows the corrected VIC measurements at km 144+926, with the estimated deviation from the head to the toe of the VIC and throughout the measurement times deducted. From the time the embankment was completed until shortly before it failed, maximum deformation always occurred at the VIC head. Between 2004 and 2017, the horizontal displacement at the upper edge of the working level increased from 86 mm to 304 mm (Figure 7), shortly before the first fracture occurred (Figure 2).

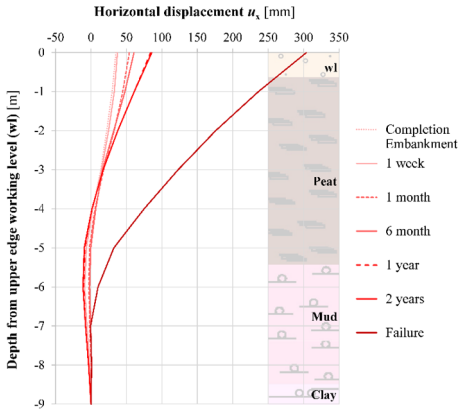

Figure 7. Corrected VIC measurements of km 144+926(A) in the failure area, starting at the upper edge of the working level

Unplanned additional loads arose due to the groundwater level dropping by up to 1 m in 2016 and the working level being thicker than planned. The underlying peat compensated for the resulting horizontal loads, leading to additional deformation, especially at the embankment toe. Another unplanned situation occurred in 2017 when a trench was excavated in the area of subsequent failure. This resulted in the vertical unloading of the edge columns, reducing their compensating bending moment. From October 4 to 7, 2017, a total of 88 mm of precipitation was recorded. Since the backfilled trench was uncovered, water flowed freely and saturated the backfill material. This caused water pressure to build up in the embankment.

5 ANALYTICAL CALCULATIONS

All stability calculations of the embankment with CSV columns indicated sufficient stability for the final state. However, it should be noted that these calculations do not consider deformations and the resulting additional stresses. In order to investigate the embankment failure in more detail, the calculation model was modified. It was assumed that the columns failed over time, starting at the toe of the embankment and progressing towards its centre. This failure can be caused by the spreading forces acting within the embankment and horizontal creep deformations in the subsoil. Column failure was simulated by successively removing them from the calculation model. Removing the first seven column rows in the slip circle calculation, resulted in failure at the embankment toe.

The VIC measurements (Figure 7) showed that the CSV columns close to the embankment toe are subject to high bending stresses. The deformation patterns resemble the bending curve of an elastically supported beam. Due to the vertical load on the columns, uniaxial bending with longitudinal force can be assumed. The flexural stresses can be calculated by considering the axial force acting on the column relative to its cross-section and the bending moment relative to the column's moment of resistance. At the point of maximum moment, the flexural stresses must not exceed the strength of the unreinforced column material. For the columns at the embankment toe, the axial force is

negligible. With an embankment height of 6 m and a load share of 90%, the axial force of a column is approx. 50 kN. A total of 75 test results yielded an average value of 5.15 N/mm² for the flexural strength of the column material. (Rackwitz et al. 2021).

Calculations were performed for various column diameters and axial forces to determine the maximum bending moment that can be compensated without failure. As this bending moment depends heavily on the column diameter, it more than doubles when comparing the planned (15 cm) and the average measured diameter (20 cm). The compensating bending moment also increases with the same flexural stress and different axial forces. Applying an axial force of 50 kN increases the bending moment that can be compensated by a factor of 1.3 compared to a zero axial force. The software GGU LATPILE (version 8.12) was used to analyze a horizontally bedded single column. Assuming that the VIC measurements represent the bending curves of the columns, the measured horizontal displacements were traced. (Figure 8).

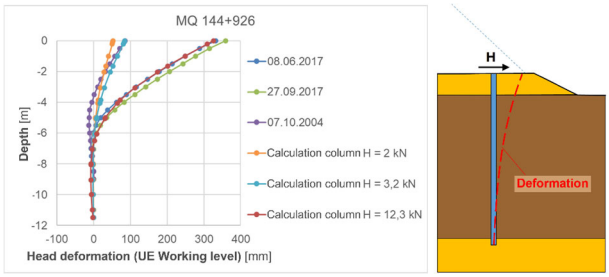

Figure 8. Measured and calculated horizontal deformations (left) and modelling (right)

Applying a horizontal point load of 2 kN to the column head results in a horizontal displacement of 53 mm. The corresponding maximum bending moment was determined as 5.4 kNm. Comparing the calculated with the compensating bending moment showed that the column cross-section with a diameter of 20 cm already failed at the determined head deformations. The measurements in the failure area exceeded the calculated value of 53 mm by the end of 2004 (Figure 7). Even if some of the columns in the edge area were already broken after two years of service, this would not necessarily lead to the failure of the entire embankment. It only becomes critical when too many columns fail, as the stability calculations showed.

6 NUMERICAL INVESTIGATIONS

To identify the causes of the BAB A 20 failure, a numerical parametric study was conducted. Numerical simulations were performed with a three-dimensional finite element (FE) model of the embankment cross-section using ANSYS® version 17.0.

6.1 *3D FE model*

The FE mesh of the basic model consists of around 263,000 elements, as shown in Figure 9 for half of the embankment cross-section (left). The ground section is 120 m long transverse to the embankment axis (X-axis) and 56 m deep from ground level (+0.7 m HN). Along the embankment axis (Z-axis), the model is 3.12 m wide, corresponding to the width of three column rows at the embankment's edge. (Figure 9)

The geometry of the embankment structure and the spacing of the CSV columns were aligned with the specifications set out in the planning and construction documents for 'Block 36' (construction km 144+900 to 144+920), which was located within the area of failure. To ensure both, a high quality FE mesh and acceptable calculating times, the circular cross-sections of the CSV columns were converted into rectangles.

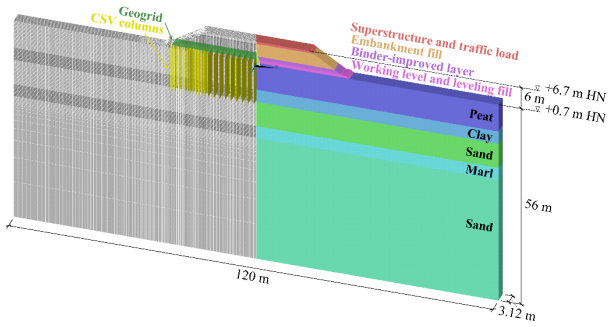

Figure 9. 3D FE model of the BAB A 20 cross-section (Y-X plane)

Figure 10 illustrates the positioning of the columns at the core and edge of the embankment in the X-Z plane for one half of the model. At the centre of the embankment, two rows of four core columns were combined into a strip to reduce computing time. The area ratio equivalence between the columns and the surrounding soil, and the bending stiffness equivalence transverse to the embankment axis, were maintained for both conversions. As specified in the planning documents, the 12.85 m long columns are embedded 1 m deep into the load-bearing sand layer beneath the soft soil.

Based on the documentation, the embankment structure is 6 m high, with a slope of 1:1.5. This gives a crest length of 26.7 m at a height of +6.7 m HN. At all vertical model boundaries, horizontal displacement normal to their plane is blocked, as is vertical displacement at the lower boundary of the model. The FE model was discretized using eight-node continuum elements (SOLID185). Only the geogrid was modelled using two-dimensional membrane elements (SHELL181).

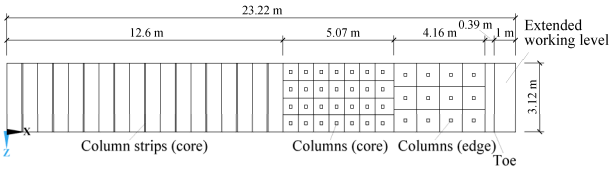

Figure 10. Spacing of the CSV columns for half of the embankment's cross-section in the X-Z plane at ground level (+0,7 m HN)

6.2 *Model structure und materials*

To simulate the creep behavior of the peat and mud layers, the anisotropic visco-hypoplasticity (AVHP) model proposed by Niemunis et al. (2009) was implemented via a user-defined subroutine. The AVHP model was developed for normally to slightly overconsolidated, viscous clays. Through its nonlinear, time-dependent formulation, the model considers creep, relaxation, rate dependence and strain-induced anisotropy. The material behavior depends on the over-consolidation ratio (OCR) as defined by Niemunis et al. (2009). In the numerical model, the soft layers of peat and mud were combined and simplified into a single layer with a thickness of 7.7 m using the material parameters of the peat from Tribsees (Table 2). An isotropic compression test with a constant strain rate (drained) and a triaxial test with varying shear rates (undrained) were carried out on reconstituted samples at TU Berlin to determine the first five values in the table. The last four parameters were estimated.

Table 2. Material parameters of the AVHP for Tribsees peat

e_{100} [/]	D_r [s^{-1}]	λ [/]	κ [/]	I_v [/]	φ_c [°]	C_1 [/]	C_2 [/]	C_3 [/]
4.2	$6.1 \cdot e^{-7}$	0.175	0.028	0.092	28	0.1	500	0.693

Oedometer tests conducted on the clay beneath the mud at TU Berlin revealed negligible creep tendencies. Therefore, the behavior of all soil layers beneath the peat was assumed to be elastoplastic using the Mohr-Coulomb (MC) failure criterion.

As planned, the working level and the leveling fill were modelled at 0.65 m and 0.2 m thick, respectively. In line with the investigations, the thickness of the binder-improved layer was reduced to a chosen value of 1 m. Due to the increased thickness of the asphalt layer in the failure area, the superstructure was considered at 0.6 m. (Chapter 3) To simplify the model, the traffic load is included as part of the superstructure's dead weight. The geogrid was modelled using linear-elastic material properties, with the stiffness values obtained from the manufacturer's datasheets. All other embankment layers were modelled as elastoplastic (MC).

The material behaviour of the rigid CSV columns was modelled using the elastoplastic 'Drucker-Prager Concrete' model. The model's strength parameters were determined from laboratory tests on recovered column remains (Chapter 3).

6.3 *Numerical simulation*

The numerical simulation reproduces the lifespan of the BAB A 20, from the start of construction to failure. The calculation steps were derived from the construction process documentation and the inclinometer measurement times. The calculation of all quasi-static load steps on the basic model took approx. 22 h on a computing server (AMD EPYC 7302P, 16 Cores, 256 GB RAM). The groundwater level was assumed to be at ground level, so that the subsoil could be considered fully saturated. For the investigation of long-term behaviour, effective soil stresses were used in the calculation. The installation of the CSV columns and the construction of the embankment were simulated as 'wished-in-place', with the dead weight of each layer applied over several days.

The initial stress of the subsoil was simulated using K0 conditions and gravity. During this first load step, the peat's material model was linear-elastic. In the next step, the model was changed to AVHP, assuming a constant initial OCR across the entire peat layer. Numerical investigations showed that subsequent application of the working level caused primary and secondary deformations that were highly sensitive to the choice of OCR. As the working level settlements are undocumented, an OCR of 2.7 was chosen. This was determined by assuming an initial void ratio of $e_0 = 12$ and a very low pseudo equivalent (preconsolidation) pressure p^{B+} close to ground level.

6.4 *Evaluation of the numerical results*

During the assessment of the BAB A 20 failure, several discrepancies between the planned and executed embankment structures were identified. By varying individual parameters in the numerical model, the influence of these factors on the load-bearing and deformation behavior can be investigated. The numerical results are evaluated by comparing them with the inclinometer measurement data (Chapter 4). For comparison with the HIC, the vertical node displacements parallel to the X-axis at +2.2 m HN were evaluated. For comparison with the VIC, the horizontal node displacements parallel to the Y-axis be between the last two rows of edge columns were evaluated. The numerical results were calculated by subtracting the displacements of the step corresponding to the zero measurement of the HIC/VIC from those of the respective step.

6.4.1 *Strength and position of the binder-improved layer*

Local inspections of the failure area revealed deviations in the thickness and position of the binder-improved layer compared to the planned values. Rather than varying the thickness of the binder-improved layer in the numerical model, its strength was changed. The influence of this change was investigated by varying the cohesion parameter c'. The effect of the layer's position was analyzed by varying the thickness d of the leveling fill.

Figure 11 shows the results of the numerical simulation for these variations compared with HIC measurements taken two years after the embankment completion. For the basic model with the planned strength ($c' = 500$ kN/m^2) and position ($d = 0.2$ m) of the binder-improved layer (blue), the settlement curve across the embankment cross-section is parabolic. This differs qualitatively from the measured curve (red), which has a sharp peak in the centre. The maximum settlement in the centre of the embankment is around 59 mm in the measurements and 50 mm in the basic model. Decreasing the strength of the binder-improved layer changes the settlement pattern. For $c' = 100$ kN/m^2 (dark green), the parabolic curve shows a plateau in the core area of the embankment. Rather than one maximum in the middle, there are two slight maxima closer to the embankment shoulders. For $c' = 50$ kN/m^2 (light green), the plateau in the core area changes to a pronounced inverted parabola. The calculated settlements at the centre of the embankment correspond to the measured values. However, in the model, the maximum settlements of 93 mm occur approx. 9 m away from the centre of the embankment. Between these maxima, the graph shows increasingly pronounced spikes towards the peaks. These indicate differences in settlement between the columns and the ground. Increasing the thickness of the leveling fill d results in a significantly different settlement pattern to that of the previous variation. Compared to the basic model, changes to the position of the binder-improved layer primarily affect the curve at the edges of the embankment. The curve remains parabolic between the embankment shoulders, but is somewhat flattened in the inner core area. At the shoulders, the settlements reach a minimum at a turning point. From these two minima, the settlements increase almost linearly towards the foot of the embankment. With an increased thickness of $d = 0.4$ m (orange), the maximum settlement at the centre of the embankment is just under 64 mm, whereas the settlement at the outer edges is approximately 41 mm. With an increased thickness of $d = 0.6$ m (yellow), the maximum settlement at the centre is 58 mm, which is almost equal to the measured value. In contrast, the settlements at the edges increase to 48 mm. Interestingly, the model with $d = 0.4$ m shows the greatest maximum settlement.

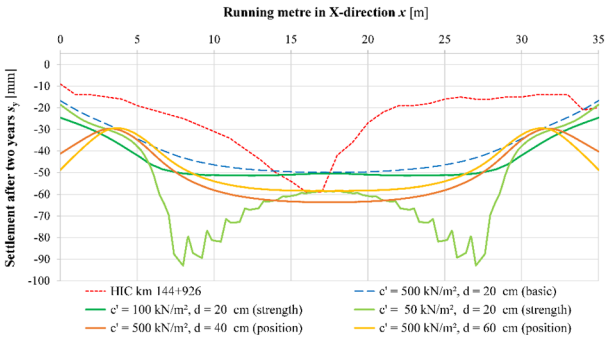

Figure 11. Comparison of HIC measurements (km 144+926) with numerical results (strength and position variation binder-improved layer)

Figure 12 illustrates how these parameter variations affect horizontal displacements at the embankment toe at the end of the calculation, which represents the time shortly before the BAB A 20 failure. The curves for variation in strength and in position of the binder-improved layer are qualitatively similar. As with the HIC measurements in the area of failure, horizontal deformation increases from the base point and reaches a maximum at the upper edge of the working level. The measurements show a significant bend in the layer transition area from mud to peat at a depth of about 5 m. Since the mud is stiffer and has a lower creep tendency than the peat, it exerts greater lateral resistance to the VIK's deformation. However, as peat and mud were combined in the model, this bending cannot be reproduced. A max-

imum calculated displacement of 186 mm is achieved with a variation of c' = 50 kN/m² (light green). This results in pronounced buckling, which is visible at the transition to the clay layer. As the material in the model changes from peat to clay, the difference in stiffness is significant, resulting in a pronounced bend. A smaller strength reduction to c' = 100 kN/m² (dark green) leads to a maximum horizontal displacement of 66 mm. In the basic model according to the planned design (blue), this is only 40 mm. Variation in the position of the binder-improved layer also led to an increase in horizontal displacements at the embankment toe. In the model with a leveling fill thickness of d = 0.4 m (orange), the maximum displacement at the upper edge of the working level is 91 mm, and for d = 0.6 m (yellow) it is 118 mm. The numerical simulations could not replicate the high measurement of 304 mm.

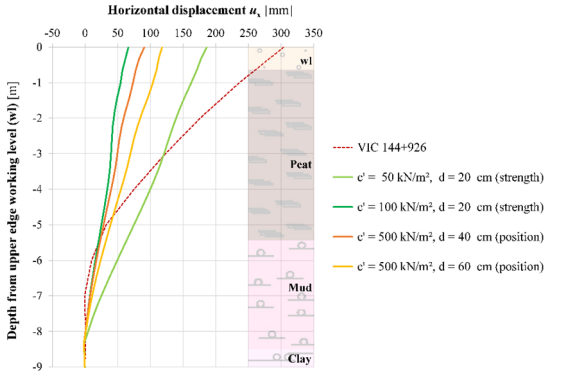

Figure 12. Comparison of VIC measurements (km 144+926) with numerical results (strength and position variation binder-improved layer)

Although the numerical results of the settlement for the two examined variations differ qualitatively from the HIC measurements at km 144+926, a comparison with other cross-sections to the west of the Trebel bridge reveals similarities for both curves (Figure 13). The measurements at km 144+516 and 144+390 exhibit characteristics similar to those of the calculated curve for the models with increased leveling fill thickness. A turning point is reached in the outer areas of these measurements, after which there is a sharp increase in settlement towards the embankment toe. Meanwhile, the measured values in the middle of the embankment at km 144+516 and 144+715 show a decrease in settlement towards the embankment axis. This corresponds to the inverse parabola in the middle of the curve for models with reduced strength in the binder-improved layer. Figure 13 also shows the settlement for combinations of changes in strength and position with c' = 100 kN/m² and d = 0.4 m (purple) and with c' = 50 kN/m² and d = 0.6 m (pink). Comparing these combined models with the VIC measurements shows that they match the settlement curve at km 144+516 qualitatively. However, the calculated maximum horizontal displacements at the upper edge of the working level are larger, at 134 mm and 336 mm respectively.

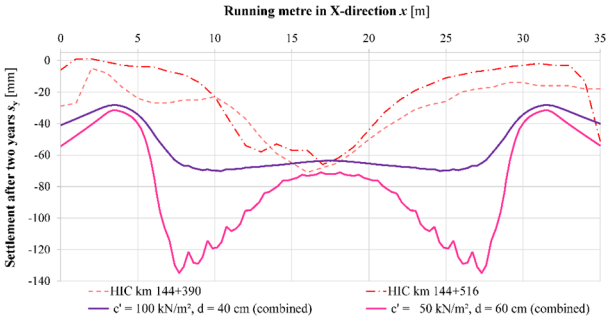

Figure 13. Comparison of different HIC measurement cross-sections with numerical results (combined variation binder-improved layer)

7 CONCLUSIONS AND OUTLOOK

To assess the failure of the BAB A20 highway near Tribsees, TU Berlin conducted an extensive investigation program, which included examining documents, performing field and laboratory tests, and running analytical and numerical calculations. The existing documentation was found to be incomplete and, somtimes contradictory to the findings from the dismantling work in the damaged area. Additionally, most of the investigations could only be conducted outside the failure area. Therefore, a wide range of influencing parameters was examined and extensive parameter studies were carried. While the investigations confirmed many of the planning assumptions, such as those relating to ground conditions and CSV column properties, some of the findings contradict the existing documentation. In most of the investigated areas, the working level was much thicker than planned, in some cases exceeding 2 m. According to the embankment dismantling documentation, the binder-improved layer was installed at insufficient thickness.

The VIC measurements indicate that the CSV columns were subjected to high bending stresses. Analytical calculations of an elastically supported beam revealed that the flexural strength of the CSV columns was insufficient to compensate for the bending moments at the embankment edge. Numerical investigations revealed that discrepancies in the planned thickness and position of the binder-improved layer lead to increased horizontal deformations at the embankment toe. This results in greater bending stress in the edge columns. The decrease in the groundwater level in 2016 and the additional water pressure from the trench in 2017, intensified the horizontal load on the columns. The first failure occurred two days after the heavy rainfall ended. Analytical stability calculations suggest that the embankment collapsed after the failure of seven column rows.

The extensively investigated failure case is ideal for calibrating and validating numerical models. The first results of further numerical investigations show that modeling an increased number of CSV columns, as documented for the failure area, yields promising results for qualitatively reproducing the HIC measurements. Future investigations will focus on the bending behavior of edge columns. However, using the AVHP results in significant deformation after the working level is applied, which is unfavorable for column installation. Additionally, the calculations significantly underestimate the large in situ creep deformations. Thus, further research into the initial state of the AVHP and the OCR is necessary. In the long term, the suitability of AVHP for organic soils must be evaluated.

Overall, the application limits of CSV columns should be defined based on subsoil conditions. Using this method in peat or mud is not recommended without restriction. Proof of horizontal deformation and suitable arrangements for practical construction testing are necessary, as well as measurement monitoring throughout the entire construction and service.

8 REFERENCES

DGGT e.V. 2002. Merkblatt für die Herstellung: Bemessung und Qualitätssicherung von Stabilisierungssäulen zur Untergrundverbesserung. Teil I – CSV-Verfahren.

Hecht, T. 2010. Bauen auf organischen Böden. Lecture at BTU Cottbus.

Niemunis, A., Grandas-Tavera, C. E., and Prada-Sarmiento, L. F. 2009. Anisotropic visco-hypoplasticity. *Acta Geotechnica* 4(4). 293–314. https://doi.org/10.1007/s11440-009-0106-3

Rackwitz, F., Aubram, D., Glasenapp, R., and Schüßler, M. 2021. Wissenschaftliche Beurteilung des Schadenfalls an der BAB A 20 bei Tribsees. Final report on the research project BASt 4500050187, TU Berlin

Scheller, P. O., and Reitmeier, W. 2001. Combined Soil Stabilization with Vertical Columns (CSV): A New Method to Improve Soft Soils. In: Hanson, J. L., and Termaat, R. J. *Soft Ground Technology*. Noordwijkerhout, 28 May – 2 June 2000. ASCE, 123-155.